SCIENTIFIC REPORTS

OPEN

SUBJECT AREAS:
METAMATERIALS
IMAGING AND SENSING
MICRO-OPTICS
TRANSFORMATION OPTICS

Received
11 October 2012

Accepted
28 May 2013

Published
12 June 2013

Correspondence and requests for materials should be addressed to G.P.W. (gp_wang@whu.edu.cn)

Directionally Hiding Objects and Creating Illusions at Visible Wavelengths by Holography

Qiluan Cheng[1], Kedi Wu[1], Yile Shi[2], Hui Wang[2] & Guo Ping Wang[1]

[1]School of Physics and Technology, Wuhan University, Wuhan 430072, Hubei, P. R. China, [2]Institute of Information Optics, Zhejiang Normal University, Jinhua 321000, Zhejiang, P. R. China.

Invisibility devices have attracted considerable attentions in the last decade. In addition to invisibility cloaks, unidirectional invisibility systems such as carpet-like cloaks and parity-time symmetric structures are also inspiring some specific researching interests due to their relatively simplifying design. However, unidirectional invisibility systems worked generally in just one certain illumination direction. Here, based on time-reversal principle, we present the design and fabrication of a kind of all-dielectric device that could directionally cancel objects and create illusions as the illuminating light was from different directions. Our devices were experimentally realized through holographic technology and could work for macroscopic objects with any reasonable size at visible wavelengths, and hence may take directional invisibility technology a big step towards interesting applications ranging from magic camouflaging, directional detection to super-resolution biomedical imaging.

Invisibility has been attracting considerable attentions in science and technology. With the development of invisibility technology, several invisibility cloaking configurations were proposed theoretically[1–10] and demonstrated experimentally[11–19] such as the invisibility cloaks that objects to be hidden were enclosed or covered by the cloaks[1–8,11–18] and complementary media (or negative-index media) -based devices used to conceal objects outside the cloaks[9]. While perfect invisibility cloaks can work independent of the position of source and observer, unidirectional invisibility devices based upon carpet-like cloaks[20] and parity-time symmetric structures[21–25] are also inspiring some specific researching interests due to their relatively simplifying design and specific application potentials in wide fields such as directional military detection and biomedical imaging etc.

Here, based on time-reversal principle[26–34], we present the design and fabrication of a kind of all-dielectric devices that could directionally cancel objects and create illusions in visible frequencies by holography[35–39]. Different from unidirectional invisibility devices, which worked generally in just one certain illumination direction, our devices could work as the incident light was from different directions and further the devices were experimentally realized with only commercially available materials (made of nonsingular, homogeneous, and isotropic materials). The objects that we used in the experiments were at the centimeter scale and the distance between the objects and the devices was at the decimeter scale.

Results

Theoretical basis and experimental scheme. Physically, to hide an object, one can employ a phase-conjugated signal to compensate for the scattered light fields of the object. While for creating optical illusions, not only is a phase-conjugated signal to compensate for the scattered light fields of one object to make it invisible needed, but further an additional light field of a different object to be transformed into must be produced[38–41]. Optically, time-reversal principle were widely exploited to produce optical phase conjugation signals in imaging beyond the diffraction limit[30,31] and focusing light into a scattering medium[32–36]. The time-reversed light beam can be created through either linear[32–36] or nonlinear optical effects[42]. In our experiments, we followed Refs. *32* and *36* to obtain time-reversed light to realize invisibility and to create illusions. The optical system used to fabricate our dielectric devices is sketched in Fig. 1a. The devices were fabricated through interference lithography by using a photosensitive plate in plane C to record the interference pattern of the coherent beams.

To construct a device (D-1) for concealing an object O_1, we placed the object in plane Q of Fig. 1a in the recording process. While to produce another device (D-2) for creating optical illusions of changing object O_1 to another object O_2, we first placed objects O_1 and O_2 in plane Q simultaneously in the exposure procedure. In our

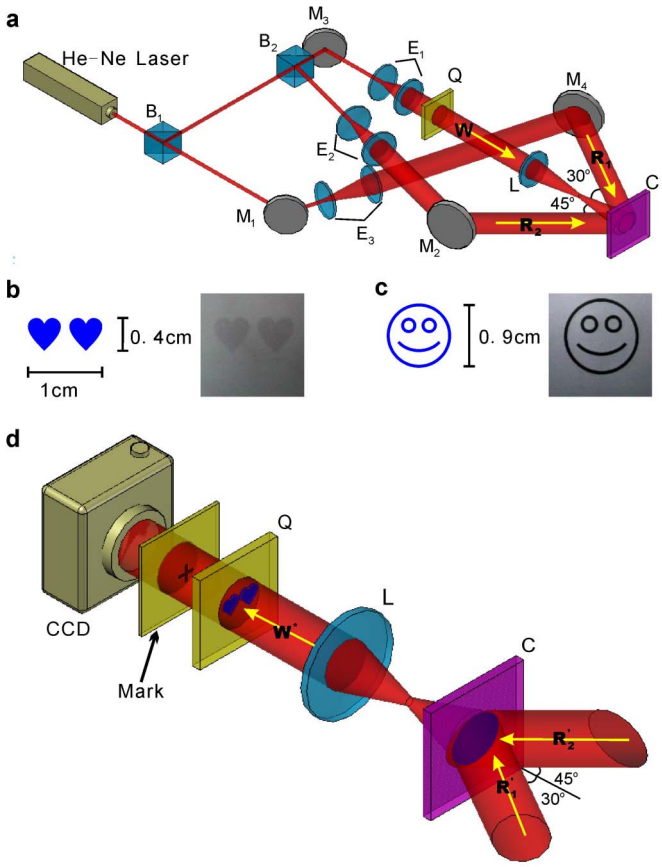

Figure 1 | Experimental setup of our dielectric devices. (a) Optical path to fabricate the devices. A He–Ne laser beam with a wavelength of λ = 632.8 nm was divided by beam splitters B_1 and B_2 into three parts: two plane-light beams R_1 and R_2 and one beam passing through an object placed in plane Q, known as the object light beam W. The angles between W and R_1 and between W and R_2 were 30° and 45° measured clockwise and anticlockwise, respectively. E_1, E_2, and E_3 were beam expanders, M_1, M_2, M_3, and M_4 were mirrors, and L was a lens with a focal distance f = 15 cm. A photosensitive plate in plane C was used to record the interference pattern of the three beams R_1, R_2, and W for constructing the devices. The distance between L and C was 30 cm, equal to the distance between L and Q, so that the object in plane Q created a one-to-one image on plane C. (b) Sketch of a transparent object O_1 and its actual image: a two-heart logo with area 1 cm × 0.4 cm. (c) Sketch of an amplitude-modulated object O_2 and its actual image: a smiling-face logo with diameter 0.9 cm. (d) Optical system used to evaluate the working effect of the devices. Each device was replaced in plane C and illuminated by a plane-light beam R_1' or R_2' on the back surface. A CCD camera was used to monitor the final output image when the plane light R_1' or R_2' passed through the devices in plane C and the object in plane Q. The distance between planes C and Q was 60 cm. The angle between the illuminating light R_1' (R_2') and the normal direction of the devices was 30° measured clockwise (45° anticlockwise). A mask plane with a cross mark was placed between the CCD and the object plane as a reference mark to monitor the effect of the devices on the nearby objects.

experiments, object O_1 was a transparent two-heart object embossed on a glass substrate, while object O_2 was an amplitude-modulated smiling face. The schemes and actual photographs of the objects are shown in Figs. 1b and 1c, respectively.

After exposure, development, fixing, bleaching, and drying (see Methods), the devices were finished. The device surface structure was a series of interference fringes (see supplementary Fig. S1 online). Since the bleaching processing makes the composites of the recording medium become a dielectric material, all devices obtained in our experiments were completely transparent (see Methods).

Figure 1d shows the optical system used to characterize the effect of the devices. To evaluate the device performance for concealing object O_1 or creating optical illusion of changing object O_1 to object O_2, we replaced the fabricated devices in plane C again and maintained the position of the object O_1 in plane Q. We then used a plane light beam to illuminate the back surface of the devices at different illuminating directions, which will produce a time-reversal light of the object light beam W used in the recording process to illuminate the object O_1 in plane Q. We observed the image behind the object O_1 through a charge-coupled device (CCD) to check the device effect. A cross mark was placed between the CCD and the object plane Q as a reference mark for monitoring the effect of the devices on nearby objects of O_1.

Characterization of D-1 in hiding objects. Figure 2a presents the photograph of object O_1 (two-heart logo, Fig. 1b) taken by CCD camera as it was directly illuminated by a laser beam at λ = 632.8 nm. The

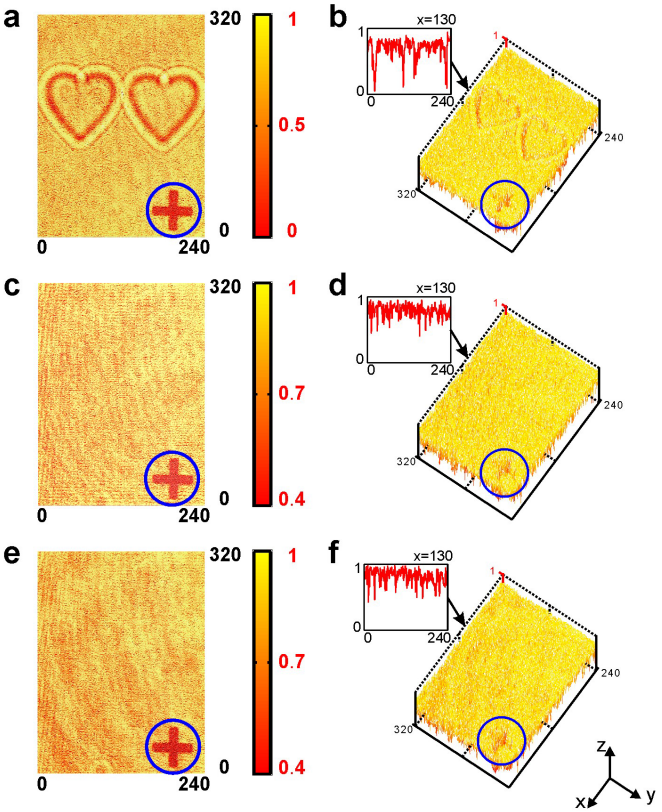

Figure 2 | Experimental results of hiding object O_1. (a) Planar photograph and (b) three-dimensional profile of object O_1 taken by CCD camera as it was directly illuminated by a laser beam at λ = 632.8 nm. Inset of (b) is the intensity distribution of the image along the y axis at x = 130. The four peaks correspond to the feature of object O_1 on the edges of two hearts. Blue-circled cross at the bottom right corner of the picture is the photograph of a cross mark placed between object O_1 and the CCD for reference. (c), (e), planar images received by the CCD when object O_1 was placed in plane Q behind D-1 and (d), (f), their three-dimensional profiles when D-1 was illuminated by [(c), (d)] R_1' at a 30° angle clockwise from the normal direction of D-1 or [(e), (f)] R_2' at a 45° angle anticlockwise from the normal direction of D-1, respectively. Insets of (d), (f) are the intensity distributions of the images along the y axis at x = 130. Note that not only can information of object O_1 hardly be seen with the exception of background noise [(c), (e)], four feature peaks of O_1 also disappear [insets of (d), (f)]. However, note that the blue-circled cross at the bottom right corner of each picture remains unchanged, indicating that D-1 did not affect the other objects around the object to be concealed.

double boundaries of two hearts appeared in the photograph are due to the diffraction effect. To quantitatively know the contrast of the photograph, we show in Fig. 2b its three-dimensional profile and in the inset the intensity distribution of the image along the y axis at $x = 130$. We can see that four peaks appear in the image, which correspond to the feature of object O_1 on the edges of two hearts. Blue-circled cross at the bottom right corner of the picture is the photograph of a cross mark placed between object O_1 and the CCD for reference.

When D-1 was inserted in plane C and illuminated by a plane light R_1' (with $\lambda = 632.8$ nm), which was separated by a 30° angle clockwise from the normal direction of D-1 (see Fig. 1d), it produced a time-reversed signal of object O_1 after passing through D-1. In this case, we again take the photograph of object O_1 by CCD camera. Figure 2c shows the planar image of the photograph. From the figure we can hardly see any information of object O_1 with the exception of background noise (caused by interference of parasitical light beams in the recording process). To get a quantitative description, we present in Fig. 2d the three-dimensional profile of the photograph, and correspondingly, in the inset the intensity distribution of the image along the y axis at $x = 130$. We see that now, unlike the inset of Fig. 2b, there are no feature peaks of object O_1 but random background noise, meaning that object O_1 was concealed and invisible.

By changing the light illuminating D-1 to R_2' (see Fig. 1d), which was at a 45° angle anticlockwise from D-1's normal direction, this also produced the other time-reversed signal of object O_1 after passing through D-1. We observed a similar phenomenon through the CCD. Figure 2e shows the planar image of the photograph. From the figure we can yet hardly see information of object O_1 with the exception of background noise. From its three-dimensional profile (Fig. 2f) and the intensity distribution of the photograph along the y axis at $x = 130$ (inset of Fig. 2f), we see that there is still no feature peak as that appears in the inset of Fig. 2b but random background noise, meaning that object O_1 was also invisible.

Note that, although the object was concealed by D-1 when illuminated in two different directions respectively, from Figs. 2c–2f we see that the cross mark placed between object O_1 and the CCD is always visible (blue-circled cross at the bottom right corner of each picture), meaning that D-1 just played the role of concealing the objects to be hidden but had no effect on other objects nearby O_1.

The movies illustrating the dynamic process of hiding the object by D-1 are provided in the supporting online materials (Movie S1a for R_1' illumination and Movie S1b for R_2' illumination).

Characterization of D-2 in creating illusions. To demonstrate the performance of D-2 in creating optical illusions, we replaced D-1 by D-2 in plane C and maintained the position of the object O_1 in plane Q. Figure 3a presents the planar photograph taken by CCD when a plane light beam R_1' (separated from the normal direction of D-2 clockwise by a 30° angle) illuminated D-2. We see that, although we only placed object O_1 in plane Q, what was visible was not object O_1 but instead an image of smiling-face logo in the same plane, Q. To get a feature properties of the image, we present in Fig. 3b the three-dimensional profile of the photograph and in the inset the intensity distribution of the image along the y axis at $x = 100$. We see that not only are there no typical peaks of object O_1 as that appeared in the inset of Fig. 2b, but instead it appears six peaks. To identify the image and the intensity peaks in Figs. 3a and 3b, we show in Fig. 3c the photograph of object O_2 (smiling-face logo, Fig. 1c) taken by CCD camera as it was directly illuminated by a laser beam at $\lambda = 632.8$ nm and in Fig. 3d its three-dimensional profile. The inset of Fig. 3d shows the intensity distribution of the photograph of object O_2 along the y axis at $x = 100$. By comparing Figs. 3a–3b and 3c–3d, we see that what we see in plane Q, where object O_1 was placed, is the image of object O_2. The six peaks appeared in the inset of Fig. 3b correspond to the feature of object O_2 on the edges of the face and two eyes of the smiling-face logo (see inset of Fig. 3d). Consequently, our results demonstrated that D-2 could not only hide object O_1 but further transfer it into another different object, O_2.

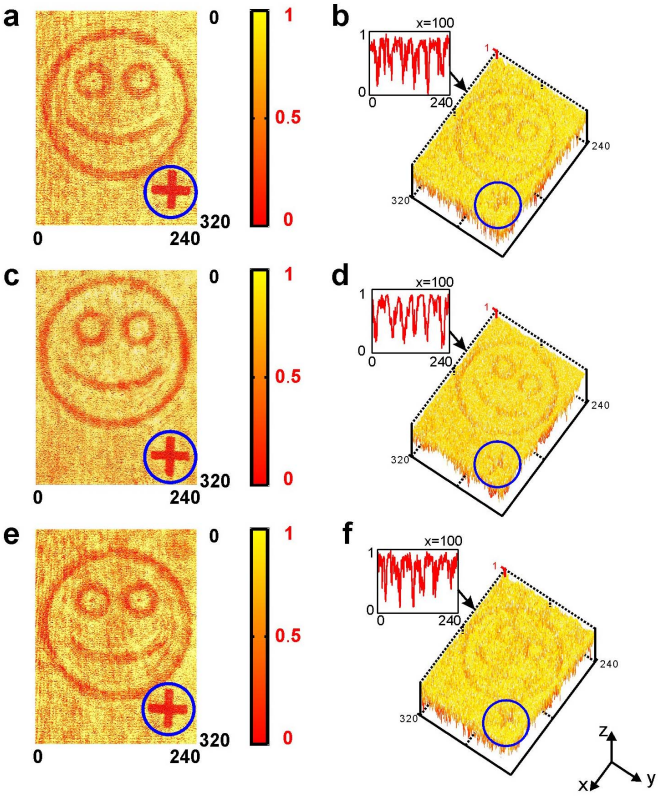

Figure 3 | Experimental results of creating an illusion of transforming object O_1 into object O_2. (a), (e), planar images received by the CCD when object O_1 was placed in plane Q behind D-2 and (b), (f) their three-dimensional profiles when D-2 was illuminated by [(a), (b)] R_1' at a 30° angle clockwise from the normal direction of D-2 or [(e), (f)] R_2' at a 45° angle anticlockwise from the normal direction of D-2, respectively. Insets of (b), (f) are the intensity distributions of the images along the y axis at x = 100. Note that not only can information of object O_1 be seen with the exception of background noise [(c), (e)], the image received by CCD is completely from another object, O_2. (c) Planar photograph and (d) three-dimensional profile of object O_2 taken by CCD camera as it was directly illuminated by a laser beam at $\lambda = 632.8$ nm. Inset of (d) is the intensity distribution of the image along the y axis at x = 100. O_2 (smiling-face logo, Fig. 1c) taken by CCD camera as it was directly illuminated by a laser beam at $\lambda = 632.8$ nm and in (d) its three-dimensional profile. The inset of (d) shows the intensity distribution of the photograph of object O_2 along the y axis at x = 100. The six peaks, which also appear in the insets of (b) and (f), correspond to the feature of object O_2 on the edges of the face and two eyes of the smiling-face logo, further confirming that D-2 plays the role of transferring O_1 into O_2. However, note that the blue- circled cross at the bottom right corner of each picture remains unchanged, indicating that D-2 did not affect the other objects around the object to be transformed.

A similar result was obtained by replacing the illuminating light beam R_1' with R_2', which was at 45° angle anticlockwise from the normal direction of D-2. The image observed through the CCD was yet not that of object O_1 (Fig. 2a) but that of object O_2 (Fig. 3e). The three-dimensional profile of the photograph (Fig. 3f) and its corresponding intensity distribution along the y axis at $x = 100$ (inset of Fig. 3f) further quantitatively confirm that there indeed are no typical peaks of object O_1 as that appeared in the inset of Fig. 2b but instead of six feature peaks of object O_2 (inset of Fig. 3d) under a certain of random background noise.

Similar to concealing object O_1 discussed before, although D-2 was efficacious in creating the optical illusion, from Figs. 3a, 3b, 3e, and 3f we see that the image of the cross mark placed between object O_1 and the CCD remains the same as that without D-2 O_1 (blue-circled cross at the bottom right corner of each picture), meaning that D-2 had no effect on the near O_1 by objects.

Note that as the illuminating light beam was R_1' and R_2', respectively, the image quality (brightness) of the photographs (Figs. 2c, 2d, 3a, and 3b for illuminating beam R_1', Figs. 2e, 2f, 3e, and 3f for beam R_2') shows slight difference. This is due to the intensity difference between the two plane lights R_1 and R_2 in the process of fabricating the devices. In addition, a careful comparison shows that the background noise in creating optical illusions of changing one object to another object (see Figs. 3a, 3b, 3e, and 3f) is more obvious than that in concealing objects (Figs. 2c–2f). This can be attributed to the fact that amplitude object O_2 shows stronger effect than phase-only object O_1 in consuming and disturbing the object light W when recording the devices.

The movies illustrating the dynamic process of creating the optical illusions by using D-2 are provided in the supporting online materials (Movie S2a for R_1' illumination and Movie S2b for R_2' illumination).

Discussion

Note that we have only considered the case in which our dielectric devices worked in monochromatic light. Although operating in broad-spectrum light was challengeable, if we were to use panchromatic holographic plates to fabricate the devices by recording the interference patterns of object light beams and other plane light beams at different wavelengths, it could be extended to work, instead of in broad-spectrum light, at multiple frequencies[37]. Alternatively, by employing round-light interference lithography, we could, at least in principle, make our devices work well when observed from 360°. Furthermore, the devices could also work under more nimble illumination and observation conditions if a number of different interference beams (plane light beams and spherical light beams for example) was used in the fabrication procedure.

It should be pointed out that, although our devices could hide macroscopic objects and create optical illusions at large distance, they should be work in a special way. Nevertheless, comparing to the unidirectional invisibility systems, in which the illumination light is generally in only one specific direction, our devices provide a more interesting and also practical way to realize distant invisibility and create illusion functions.

To traditional holography, the depth limitation of holographic "anti-image" is related to the coherence length of the laser light[43], which in our experiment was about 30 cm. This means that, in principle, the greatest value of optical thickness (product of geometric thickness and refractive index) of the objects used in our case was 30 cm. Nevertheless, to experimentally reach a high quality of hiding objects and creating illusions, where the objective waves and time-reversal signals must be conjugated with each other exactly, we just used two thin objects in the experiments. The thickness difference between the two-heart area and the other areas of object O_1 was 3 μm, and the glass substrate was 1.1 mm thick, while the thickness of object O_2 was 1.1 mm. On the other hand, although in theory time-reversal signals must exactly match the object light, our devices still worked well experimentally as a slight deviation of illumination light from its conjugation light was existed. These may be attributed to the fact that aberration produced by the mismatching could be buried by the noise environment created in experiments. For instance, when our devices were illuminated by light beams R_1' or R_2' (from two different directions, 75 degrees away from each other), the maximum deviation angle of illuminating light beam depended on the diffraction effect of our devices and diameter of the imaging lens L. Thus, in our case of the diameter of the imaging lens being 7 cm, the maximum deviation angle was around 5°. For beam divergence, the maximum allowable value of divergence angle was about 1°, which can be increased further in principle if the distance between the beam expander E_1 and imaging lens L (see Fig. 1 a) is long enough. Therefore, along the illuminating directions of light (R_1' and R_2' in our experiments), the maximum allowable beam divergence angle and maximum deviation angle of the illuminating beam were about 1 and 5 degrees, respectively. Additionally, we also tested the properties of our devices in hiding object as the illuminating light was with wavelength $\lambda = 532$ nm (different from $\lambda = 632.8$ nm we used in the recording process). The result shows that our devices still achieved invisibility effect. In addition to noise, this may also be due to the fact that the object we used was so large that the spatial frequencies were very low to easily be matched. For axial deviation of object and time-reversal devices, the maximum off-axis deviation of the devices was about 25 μm as object was fixed. Larger deviation than 25 μm would destroy working effect of our devices in hiding O_1 or transforming O_1 into O_2 (see supplementary Fig. S2 online).

In conclusion, we have, based on time-reversal principle, demonstrated the all-dielectric devices to directionally hide objects and create illusions at visible wavelengths (with a wavelength of $\lambda = 632.8$ nm used in the experiments here). On the one hand, the time-reversed light produced by the devices could completely compensate for the scattered light of a macroscopic object to make the object invisible. On the other hand, a device containing additional information of another object could further create optical illusions whereby one sees a hidden object as another object, even when the object was illuminated by light beams from different directions (with two directions chosen in our present experiments). The objects that we used in the experiments were macroscopic, with sizes at the centimeter scale. The distance between the object and the dielectric devices was at the decimeter scale (with 60 cm chosen in our experiments). Comparing to the unidirectional invisibility systems, in which the illumination light is generally in only one specific direction, our devices provide a more interesting and also practical way to realize distant invisibility and create illusion functions, and hence may take directional invisibility devices a big step towards interesting applications ranging from magic camouflaging to super-resolution biomedical imaging and sensing.

Methods

To create object O_1, we first printed two opaque heart-shaped pictures on a transparent film, and then used it as a mask to expose the holographic recording plate by the He–Ne laser (with $\lambda = 632.8$ nm). After exposure, the tiny silver halide grains suspended in the gelatin were photo reduced into small silver particles in the areas exposed to light. When the exposed plate was immersed in developer D-19 for development, the silver halide crystals around the photo reduced silver particles, which were regarded as development centers, would further be chemically reduced to metallic silver. By bleaching the developed plate in an aqueous mercuric chloride solution, the reduced silver particles in the exposed areas became a silver compound. Then the plate was illuminated by a mercury vapor lamp to remove mercury ions. To remove the unreduced silver halide crystals, the plate was then fixed by an F-5 solution. In this process, the silver compound in the exposed areas was re-reduced to silver particles again. After being bleached by a diluted R-10 solution, the reduced metallic silver particles were re-oxidized into tiny silver halide grains, which was a dielectric material. Consequently, a phase-only object O_1 with low light absorption was obtained (see Fig. 1b). (For detailed postprocessing procedures and formulas for different postprocessing solutions, refer to supplementary materials and Ref. *37*.).

To fabricate object O_2, a transparent smiling-face picture printed on a black film was used as a mask to expose a holographic recording plate. All the other postprocessing procedures were the same as those for creating object O_1 but without the two bleaching steps. Hence O_2 was an amplitude-modulated object (Fig. 1c).

The postprocessing of D-1 and D-2 was almost the same as that for creating object O_1 but without the bleaching step using aqueous mercuric chloride. As a result, the devices we obtained were constructed with all-dielectric materials with high transparency (see supplementary Figs. S1a and S1b online). The micrographs shown in Supplementary Figures S1c and S1d revealed that the surface structures of D-1 and D-2 respectively were a series of interference fringes formed by object light W and two plane-light beams R_1 and R_2.

To evaluate the device performance for concealing an object (O_1) and creating illusions (transferring object O_1 into object O_2), a CCD camera was used to monitor and record the dynamic process as objects were first directly illuminated by plane

light and then D-1 and D-2 (controlled by a step motor with 2.5 μm/step) were gradually inserted between the object plane and the light source, respectively. The illuminating light beams R_1' and R_2' with $\lambda = 632.8$ nm were from two different incident directions.

1. Pendry, J. B., Schurig, D. & Smith, D. R. Controlling electromagnetic fields. *Science* **312**, 1780–1782 (2006).
2. Leonhardt, U. Optical conformal mapping. *Science* **312**, 1777–1780 (2006).
3. Chen, H., Chan, C. T. & Sheng, P. Transformation optics and metamaterials. *Nat. Mater.* **9**, 387–396 (2010).
4. Danner, A. J., Tyc, T. & Leonhardt, U. Controlling birefringence in dielectrics. *Nat. Photon.* **5**, 357–359 (2011).
5. Alu, A. & Engheta, N. Multifrequency optical invisibility cloak with layered plasmonic shells. *Phys. Rev. Lett.* **100**, 113901 (2008).
6. Ruan, Z., Yan, M., Neff, C. W. & Qiu, M. Ideal cylindrical cloak: perfect but sensitive to tiny perturbations. *Phys. Rev. Lett.* **99**, 113903 (2007).
7. Cai, W., Chettiar, U. K., Kildishev, A. V. & Shalaev, V. M. Optical cloaking with metamaterials. *Nat. Photon.* **1**, 224–227 (2007).
8. Li, J. & Pendry, J. B. Hiding under the carpet: a new strategy for cloaking. *Phys. Rev. Lett.* **101**, 203901 (2008).
9. Lai, Y., Chen, H. Y., Zhang, Z.–Q. & Chan, C. T. Complementary media invisibility cloak that cloaks objects at a distance outside the cloaking shell. *Phys. Rev. Lett.* **102**, 093901 (2009).
10. Lai, Y. *et al*. Illusion optics: the optical transformation of an object into another object. *Phys. Rev. Lett.* **102**, 253902 (2009).
11. Schurig, D. *et al*. Metamaterial electromagnetic cloak at microwave frequencies. *Science* **314**, 977–980 (2006).
12. Liu, R. *et al*. Broadband ground-plane cloak. *Science* **323**, 366–369 (2009).
13. Valentine, J., Li, J., Zentgraf, T., Bartal, G. & Zhang, X. An optical cloak made of dielectrics. *Nat. Mater.* **8**, 568–571 (2009).
14. Gabrielli, L. H., Cardenas, J., Poitras, C. B. & Lipson, M. Silicon nanostructure cloak operating at optical frequencies. *Nat. Photon.* **3**, 461–463 (2009).
15. Ergin, T., Stenger, N., Brenner, P., Pendry, J. B. & Wegener, M. Three-dimensional invisibility cloak at optical wavelengths. *Science* **328**, 337–339 (2010).
16. Fischer, J., Ergin, T. & Wegener, M. Three-dimensional polarization-independent visible-frequency carpet invisibility cloak. *Opt. Lett.* **36**, 2059–2061 (2011).
17. Chen, X. *et al*. Macroscopic invisibility cloaking of visible light. *Nat. Commun.* **2**, 176 (2011).
18. Zhang, B., Luo, Y., Liu, X. & Barbastathis, G. Macroscopic invisibility cloak for visible light. *Phys. Rev. Lett.* **106**, 033901 (2011).
19. Li, C. *et al*. Experimental realization of a circuit-based broadband illusion-optics analogue. *Phys. Rev. Lett.* **105**, 233906 (2010).
20. Landy, N. & Smith, D. R. A full-parameter unidirectional metamaterial cloak for microwaves. *Nat. Mater.* **12**, 25–28 (2012).
21. Lin, Z. *et al*. Unidirectional invisibility induced by PT-symmetric periodic structures. *Phys. Rev. Lett.* **106**, 213901 (2011).
22. Longhi, S. Invisibility in PT-symmetric complex crystals. *J. Phys. A* **44**, 485302 (2011).
23. Jones, H. F. Analytic results for a PT-symmetric optical structure. *J. Phys. A* **45**, 135306 (2012).
24. Miri, M. A., Regensburger, A., Peschel, U. & Christodoulides, D. N. Optical mesh lattices with PT symmetry. *Phys. Rev. A* **86**, 023807 (2012).
25. Feng, L. *et al*. Experimental demonstration of a unidirectional reflectionless parity-time metamaterial at optical frequencies. *Nat. Mater.* **12**, 108–113 (2013).
26. He, G. S. Optical phase conjugation: principles, techniques, and applications. *Prog. Quant. Electron.* **26**, 131–191 (2002).
27. Fink, M. *et al*. Time-reversed acoustics. *Rep. Prog. Phys.* **63**, 1933–1995 (2000).
28. Tourin, A., Van Der Biest, F. & Fink, M. Time reversal of ultrasound through a phononic crystal. *Phys. Rev. Lett.* **96**, 104301 (2006).
29. Resch, K. J. *et al*. Time-reversal and super-resolving phase measurements. *Phys. Rev. Lett.* **98**, 223601 (2007).
30. Pendry, J. B. Time reversal and negative refraction. *Science* **322**, 71–73 (2008).
31. Lerosey, G., De Rosny, J., Tourin, A. & Fink, M. Focusing beyond the diffraction limit with far-field time reversal. *Science* **315**, 1120–1122 (2007).
32. Xu, X., Liu, H. & Wang, L. V. Time-reversed ultrasonically encoded optical focusing into scattering media. *Nat. Photon.* **5**, 154–157 (2011).
33. Wang, Y., Judkewitz, B., DiMarzio, C. A. & Yang, C. Deep-tissue focal fluorescence imaging with digitally time-reversed ultrasound-encoded light. *Nat. Commun.* **3**, 928 (2012).
34. Judkewitz, B., Wang, Y., Horstmeyer, R., Mathy, A. & Yang, C. Speckle-scale focusing in the diffusive regime with time reversal of variance-encoded light (TROVE). *Nat. Photon.* **7**, 300–305 (2013).
35. Kogelnik, H. Holographic image projection through inhomogeneous media. *Bell System Tech. J.* **44**, 2451 (1965).
36. Yaqoob, Z., Psaltis, D., Feld, M. S. & Yang, C. Optical phase conjugation for turbidity suppression in biological samples. *Nat. Photon.* **2**, 110–115 (2008).
37. Goodman, J. W. *Introduction to Fourier Optics* (McGraw-Hill, New York, ed. 3 2005).
38. Wu, K., Cheng, Q. & Wang, G. P. Fourier optics theory for invisibility cloaks. *J. Opt. Soc. Am. B* **28**, 1467–1474 (2011).
39. Cheng, Q., Wu, K. & Wang, G. P. All dielectric macroscopic cloaks for hiding objects and creating illusions at visible frequencies. *Opt. Express* **19**, 23240–23248 (2011).
40. Wu, K. & Wang, G. P. General insight into the complementary medium-based camouflage devices from Fourier optics. *Opt. Lett.* **35**, 2242–2244 (2010).
41. Wu, K. & Wang, G. P. Hiding objects and creating illusions above a carpet filter using a Fourier optics approach. *Opt. Express* **18**, 19894–19901 (2010).
42. Longhi, S. Time-reversed optical parametric oscillation. *Phys. Rev. Lett.* **107**, 033901 (2011).
43. Kreis, T. *Handbook of holographic interferometry optical and digital methods* (Wiley-VCH, 2004).

Acknowledgements

We thank Prof. C. J. Dong from the University of St. Andrews for valuable comments and suggestions. This work is supported by the 973 Program (2011CB933600), the NSFC (Grants 60925020 and 11274247). K.D.W. is also supported by the Academic Award for Excellent Ph.D. Candidates funded by the Ministry of Education of China (Grant 5052011202009).

Author contributions

Q.L.C. performed the experiments, K.D.W. performed the theoretical analysis, Y.L.S. assisted the experiments, H.W. and G.P.W. designed and conducted the experiments, G.P.W. conceived the idea and supervised the project. All authors contributed to the final version of the manuscript.

Additional information

Supplementary information accompanies this paper at http://www.nature.com/scientificreports

Competing financial interests: The authors declare no competing financial interests.

How to cite this article: Cheng, Q., Wu, K., Shi, Y., Wang, H. & Wang, G.P. Directionally Hiding Objects and Creating Illusions at Visible Wavelengths by Holography. *Sci. Rep.* **3**, 1974; DOI:10.1038/srep01974 (2013).